Research Paper

Reduced signal propagation elicited by frontal transcranial magnetic stimulation is associated with oligodendrocyte abnormalities in treatment-resistant depression

Masataka Wada, MD; Shinichiro Nakajima, MD, PhD; Shiori Honda, MSc; Mayuko Takano, MSc; Keita Taniguchi, BSc; Sakiko Tsugawa, MD; Yu Mimura, MD; Nanao Hattori; Shinsuke Koike, MD, PhD; Reza Zomorrodi, PhD; Daniel M. Blumberger, MD, MSc; Zafiris J. Daskalakis, MD, PhD; Masaru Mimura, MD, PhD; Yoshihiro Noda, MD, PhD, MBA

Background: The efficacy of repetitive transcranial magnetic stimulation (rTMS) to the left dorsolateral prefrontal cortex (dlPFC) has been established in patients with treatment-resistant depression (TRD), suggesting that alterations in signal propagation from the left dlPFC to other brain regions may be linked to the pathophysiology of TRD. Alterations at the cellular level, including dysfunction of oligodendrocytes, may contribute to these network abnormalities. The objectives of the present study were to compare signal propagation from the left dlPFC to other neural networks in patients with TRD and healthy controls. We used TMS combined with electroencephalography to explore links between cell-specific gene expression and signal propagation in TRD using a virtual-histology approach. **Methods:** We examined source-level estimated signal propagation from the left dlPFC to the 7 neural networks in 60 patients with TRD and 30 healthy controls. We also calculated correlations between the interregional profiles of altered signal propagation and gene expression for 9 neural cell types derived from the Allen Human Brain Atlas data set. **Results:** Signal propagation from the left dlPFC to the salience network was reduced in the θ and α bands in patients with TRD ($p = 0.0055$). Furthermore, this decreased signal propagation was correlated with cell-specific gene expression of oligodendrocytes ($p < 0.000001$). **Limitations:** These results show only part of the pathophysiology of TRD, because stimulation was limited to the left dlPFC. **Conclusion:** Reduced signal propagation from the left dlPFC to the salience network may represent a pathophysiological endophenotype of TRD; this finding may be associated with reduced expression of oligodendrocytes.

Introduction

Major depressive disorder (MDD) is one of the most prevalent mental disorders.[1] However, nearly one-third of patients with MDD show little or no response to 2 or more antidepressant medications, a condition that is termed treatment-resistant depression (TRD).[2] Patients with TRD have a lower quality of life, greater impairment of work productivity and increased use of health care resources compared to treatment responders.[3] There is an urgent need to elucidate the pathophysiology of TRD to develop novel, effective therapies.

A host of studies using functional MRI and resting-state electroencephalography have contributed to our understanding of the pathophysiology of MDD.[4] Recent studies using resting-state functional MRI have revealed that patients with MDD have abnormal activity in the default mode, salience and frontoparietal networks.[5] In contrast, few studies have comprehensively evaluated network anomalies in patients with TRD on a large scale. Although previous studies have demonstrated abnormal activity in the default mode and salience networks in patients with TRD compared to treatment responders, these studies have shown inconsistent findings, including a mixture of hyperactivity and hypoactivity.[6,7]

On the other hand, repetitive transcranial magnetic stimulation (rTMS) to the left dorsolateral prefrontal cortex (dlPFC) is an established treatment for TRD, providing insight into a

Correspondence to: Y. Noda and S. Nakajima, Department of Neuropsychiatry, Keio University School of Medicine, 35 Shinanomachi, Shinjuku, Tokyo 160-8582, Japan; yoshi-tms@keio.jp, shinichiro_nakajima@hotmail.com

Submitted May 28, 2022; Revised Jul. 7, 2022; Accepted Jul. 10, 2022

Cite as: *J Psychiatry Neurosci* 2022 September 14;47(5). doi: 10.1503/jpn.220102

pathophysiological basis for TRD.[8] Alkhasli and colleagues[9] showed that rTMS over the left dlPFC altered the connectivity between the left dlPFC and other brain structures, including the striatum and amygdala, as well as other cortices. Other studies have indicated that connectivity between the left dlPFC and the subgenual anterior cingulate cortex could predict the efficacy of rTMS to the dlPFC in TRD.[10,11] Moreover, Godfrey and colleagues[12] demonstrated that rTMS for TRD reduced activity in the salience network. These findings suggest that alterations within and between functional connectivity networks from the left dlPFC to other brain regions may contribute to the pathophysiology of TRD.

Attention is being paid to the pathophysiology seeded by the dlPFC in patients with TRD; however, challenges in elucidating TRD-specific pathophysiology may be the result of difficulties in conducting clinical studies limited to TRD — both in terms of recruitment and in the limitations of analytical techniques in studies that use functional connectivity as an indicator. Recent functional connectivity studies have employed resting-state or task-based functional MRI or electroencephalography (EEG), but these measures assess endogenous brain activity, making it difficult in principle to examine brain activity in specific regions. In addition, Smart and colleagues[13] noted that deep brain stimulation to the subcallosal cingulate increased α power and decreased β power at the site of stimulation, implying that activity at each frequency band may have a distinct neurophysiological mechanism and function. To elucidate the pathophysiology of TRD, it is crucial to quantitatively evaluate how signal propagation from the dlPFC (the site of rTMS) to other brain regions is neuromodulated, and to investigate the characteristics related to its frequency modulation.

In this context, concurrent TMS-EEG measurement is a promising modality that can be used to measure such causal network activity in the human cortex in a noninvasive manner. TMS-EEG is a novel method of assessing brain function; it works by stimulating a target area with TMS (which strictly limits the extent of spatial activation, affecting cortical spike activity in an area less than 2 mm in diameter) and measuring the response using EEG.[14,15] It enables the measurement of how firing of the area stimulated by TMS spreads to other brain areas (i.e., signal propagation from one area to others).[14,16–18] This method has been applied successfully in previous studies: for example, to detect and evaluate network changes in the sleep–wake state, as well as in consciousness disorders.[19,20] Furthermore, Ozdemir and colleagues[21] have shown that TMS to specific brain regions could activate remote brain regions via specific neural networks using TMS-EEG. In this way, TMS-EEG is a suitable method for evaluating the network-specific signal propagation of each frequency band from the dlPFC to other brain areas.

A recent study indicated that rTMS increased the number of oligodendrocytes in the cerebral cortex of adult mice, suggesting that oligodendrocyte dysfunction may contribute to network abnormalities.[22] As a molecular basis for TRD, alterations at the cellular level may be associated with impaired signal propagation from the left dlPFC to other brain regions.[23] To date, no study has examined the relationship between EEG signal propagation and gene expression at the cellular level in patients with TRD.[24–26] Determining which cell-specific changes are responsible for impaired signal propagation would shed new light on the pathogenesis of TRD.

In the present study, our primary objective was to evaluate differences in signal propagation from the left dlPFC to other brain regions in patients with TRD compared to healthy controls; to do this, we applied time–frequency analysis to TMS-evoked potentials (TEPs). Our hypothesis was that the signal propagation from the left dlPFC to other brain regions (especially in the default mode, salience and frontoparietal networks) would be altered in patients with TRD compared to healthy controls. Our secondary objective was to explore the relationships between TEP-derived altered signal propagation and gene expression levels (variations in the expression of genes marking specific cell types) in patients with TRD using a virtual-histology approach.[27,28] We hypothesized that abnormalities in the signal propagation of TEPs would be associated with variations in the gene expression profiles of specific cells, such as oligodendrocytes.

Methods

Participants

The present cross-sectional study was conducted at Keio University Hospital between 2017 and 2022. All participants provided written informed consent according to the Declaration of Helsinki, and the protocol was approved by the ethical committee at Keio University School of Medicine. The study included patients aged 18 years or older who were treated in regular clinical practice at Keio University Hospital. Patients met the inclusion criteria if they had a diagnosis of MDD based on the DSM-5.[29] Exclusion criteria and criteria for TRD are described in Appendix 1, available at www.jpn.ca/lookup/doi/10.1503/jpn.220102/tab-related-content. Because all participants in the present study were scheduled to participate in another clinical trial (jRCT 032180188) that required adjustment of antidepressant medication, all patients with TRD were unified on venlafaxine (150 mg/d to 225 mg/d), and all other antidepressants were tapered and discontinued, with a 4-week lead-in period that included safety monitoring for adverse events. Healthy controls met inclusion criteria if they had no history of psychiatric illness (confirmed by psychiatrists).

The patient and healthy control groups were matched as closely as possible for age (within 5 years) and sex. We calculated the sample size based on a previous study that compared TMS-EEG indices between patients with MDD and healthy controls.[30] The ratio of the TRD and healthy control groups was adjusted to 2:1 for recruitment considerations. In the present study, we determined that 60 participants in the TRD group and 30 participants in the healthy control group would provide at least 80% power to detect the expected difference in TMS-EEG indices at $\alpha = 0.05$.

Clinicodemographic assessments

We obtained clinical information (including medical history and years of education) by interview. Trained psychiatrists and clinical psychologists assessed participants' severity of depression using the Montgomery–Åsberg Depression Rating Scale.

Study design

A conceptual diagram of how we combined TMS-EEG and MRI data to evaluate signal propagation and its relationship to human brain gene expression is provided in Figure 1.

MRI data acquisition

Procedural details for MRI data acquisition are described in Appendix 1.

TMS administration

TMS was delivered using a monophasic TMS stimulator (DuoMAG MP; Deymed Diagnostic Ltd.) and a figure-8 butterfly coil with 2 × 70 mm diameter windings (DuoMAG 70BF; Deymed Diagnostic Ltd.). All participants received 80 instances of single-pulse TMS at a stimulus intensity of 120% of the resting motor threshold, with the coil positioned at 45° to the midline during stimulation. Other details are provided in Appendix 1. TMS is considered safe in humans, as demonstrated by comprehensive studies of potential adverse effects and complications.[32]

EEG recording and preprocessing

EEG was recorded on the patient's scalp at a sampling rate of 3 kHz by a TMS-compatible 64-channel EEG amplifier equipped with a sample-and-hold circuit system and an EEG cap with silver cling electrodes (TruScan LTl; Deymed Diagnostic Ltd.). All electrodes were referenced to an electrode connected to the right earlobe, and the ground electrode was set on the left earlobe. The impedance between the scalp and electrodes was kept below 5 kΩ throughout the experiments.

EEG data were processed using EEGLAB v2021.0 and customized scripts running in MATLAB (R2020a; MathWorks Inc.)[33] and TMS-EEG Signal Analyzer (TESA v1.1.1).[34] Other details are provided in Appendix 1.

EEG data analysis

Sensor-based EEG analysis

We performed sensor-based EEG analysis using minimum norm estimate software.[35] We calculated global mean field power (GMFP) at the participant level for each group by subtracting the mean potential of all electrodes from the potential of each electrode; dividing the sum of squares by the number of electrode channels; and then taking the square root. GMFP represents the standard deviation between the potentials of all electrode channels and is used to assess the global brain response to TMS over the left dlPFC.[36,37] We also calculated local mean field power (LMFP; an index of local responsiveness) corresponding to the dlPFC site (average of F3, F5 and AF3 electrode sites) using the same procedure as for the GMFP calculation.[38]

To examine the TMS-elicited oscillatory characteristics when single-pulse TMS was applied to the dlPFC, we calculated event-related spectral perturbation (ERSP) and evoked power with time–frequency analyses. ERSP indicates the time-locked spectral activity elicited by TMS in power relative to a prestimulus baseline. Evoked power indicates the phase-locked spectral activity elicited by TMS in power relative to a prestimulus baseline. We calculated ERSP by averaging each power over epochs at given channel-frequency time points using open-source minimum norm estimate software (tfr_morlet), implemented with Morlet wavelets ranging from 3 to 10 cycles. We calculated evoked power in the same manner after averaging the data across trials for each electrode. Then, we baseline-corrected ERSP and evoked power (–500 to –100 ms) and converted them to logarithmic ratios. For ERSP and evoked power, we also calculated the overall mean value and the dlPFC stimulation site value (average of F3, F5 and AF3 electrode sites).

Source-based EEG analysis

We performed all TMS-evoked EEG source reconstruction using minimum norm estimate software;[35] details are provided in Appendix 1. We applied group-level functional parcellations and confidence maps estimated from 1000 healthy participants, based on a 7-network cortical parcellation that corresponded to the visual, somatomotor, limbic, dorsal attention, salience, default mode and frontoparietal networks.[32] The EEG source reconstruction resulted in the output of dynamic statistical parametric mapping (dSPM) current density time series for each network.

To investigate TMS-elicited oscillatory characteristics in each network, we performed a time–frequency analysis in the manner used to estimate ERSP and evoked power for each network (described above).

Statistical analysis for EEG analysis

We performed all statistical analyses using minimum norm estimate software.[35] To compare the time series of GMFP, LMFP and network-based dSPM current density between the 2 study groups, we performed a 1-dimensional cluster-level statistical permutation test (permutation $n = 10000$)[39,40] with a time window of 30 to 500 ms after TMS. For time–frequency analysis, we performed a 2-dimensional cluster-level statistical permutation test (permutation $n = 10000$)[39,40] with a time window of 30 to 500 ms after TMS and a frequency window of 4 to 50 Hz. We applied Bonferroni correction to control for multiple comparisons. We set the significance level for sensor-based EEG analysis at $\alpha = 0.05$ for GMFP and LMFP, and at $\alpha = 0.0071$ (0.05/7 networks) for the source-based EEG analysis.

Cell-specific gene expression analysis and statistical analysis

We conducted cell-specific gene expression analysis using postmortem brain data generated from 6 healthy donors in the Allen Human Brain Atlas genetics data set.[41] We mapped average gene expression data from the 6 donors to 34 regions in the Desikan–Killiany atlas.[42] We performed the analysis according

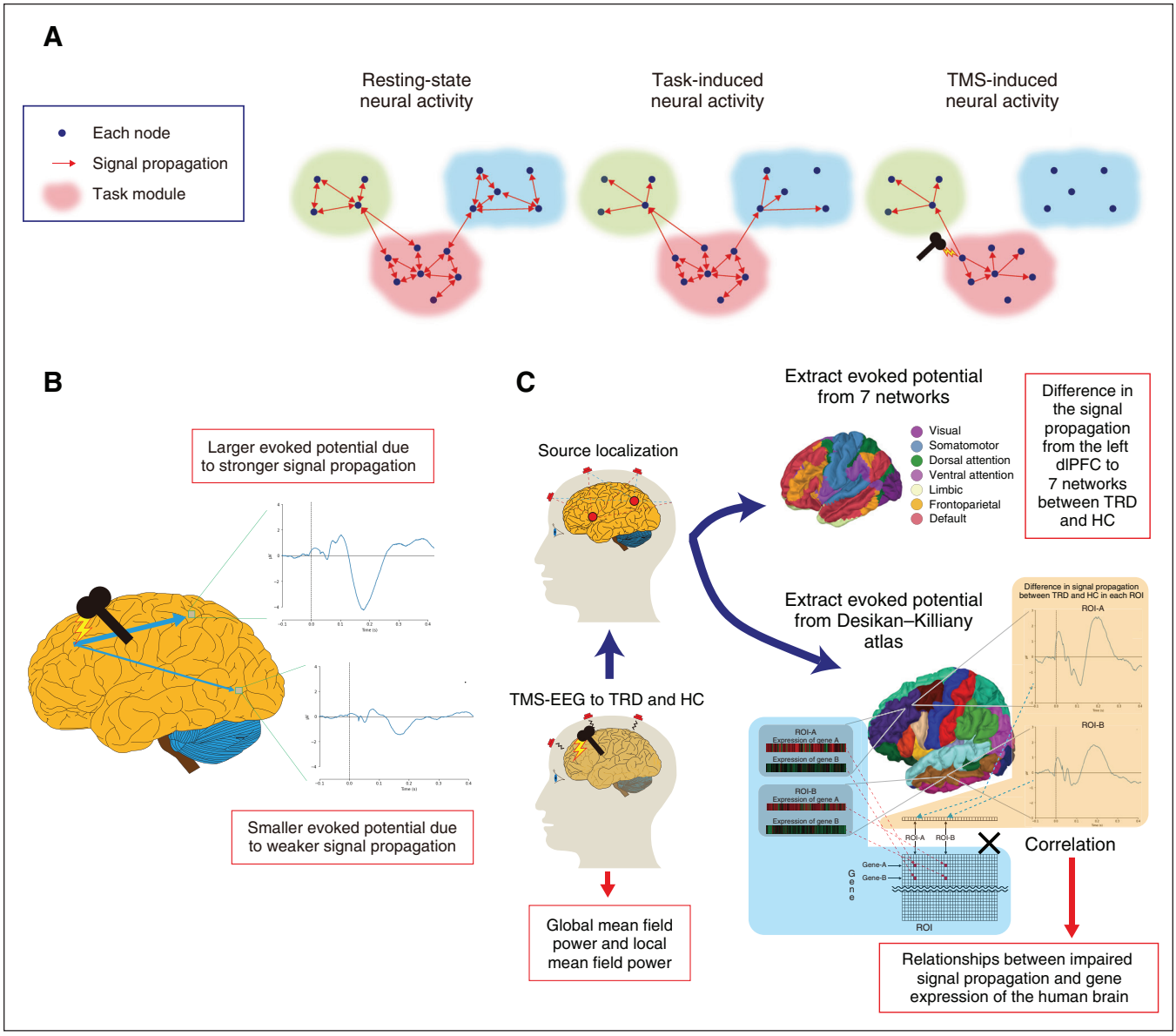

Fig. 1: Schematic diagram showing how combined TMS-EEG and MRI data were used to assess signal propagation in this study. (A) Brain neural activities comprise 3 main categories: noncausal correlated activity in the resting state; neural activity elicited by a specific task, which is assessed with endogenous neural activity specific to the task modality, elicited in the specific neural module corresponding to the task; and causal neural activity with a clear input–output relationship using an external mechanical physical stimulus as a probe. The first 2 categories have a limitation: although they can be used to evaluate local activity as the sum of the interactions between regions in the entire brain, they cannot be used to evaluate activity in the local brain region itself. The third category (extrinsic neural stimulation targeting specific brain regions using TMS as a probe) is characterized by its ability to evaluate both neural activity at the stimulation site and neural activity originating from the stimulation site to other regions to determine causal relationships, independent of neural activity from regions other than the stimulation site. (B) Rationale for using TMS-EEG to assess signal propagation in the present study. TMS-evoked neural activities (within and between regions) that show significant signal propagation from the stimulation site to other specific brain regions or neural networks are propagated in a causal manner. (C) An overview of TMS-EEG data analysis. First, for reconstruction of the TEP signal source, we manually registered EEG channel locations on individual MRI spaces, along with anatomic landmarks. Then, we projected EEG source activations onto individual surface spaces using forward and inverse modelling of EEG sources. Finally, to compare signal propagation from the stimulation site to each brain network between the TRD and healthy control groups, we extracted dSPM current densities from the 7 networks defined by Yeo and colleagues.[31] To investigate the cellular-level abnormalities that would be associated with the signal propagation abnormalities, we examined correlations between the interregional profiles of cell-specific gene expression using the Allen Human Brain Atlas data set and the interregional profiles of altered signal propagation from our TMS-EEG data. dlPFC = dorsolateral prefrontal cortex; dSPM = dynamic statistical parametric mapping; EEG = electroencephalography; HC = healthy control; ROI = region of interest; TEP = TMS-evoked potential; TMS = transcranial magnetic stimulation; TRD = treatment-resistant depression.

Table 1: Participant demographics

Characteristic*	Patients with TRD $n = 60$	Healthy controls $n = 30$	Statistics†
Age, yr	45.37 ± 11.85	45.63 ± 13.16	$t_{88} = 0.096$, $p = 0.92$
Female, %	40	40	$\chi^2_{88} = 0.0$, $p = 1.0$
Education, yr	15.3 ± 1.9	14.7 ± 2.1	$t_{88} = 1.50$, $p = 0.14$
MMSE score	29.1 ± 1.4	28.5 ± 3.3	$t_{88} = 1.38$, $p = 0.17$
Age at onset of TRD, yr	36.0 ± 15.6	—	—
Duration of illness, yr	10.9 ± 9.2	—	—
MADRS score	32.1 ± 7.1	—	—

MADRS = Montgomery–Åsberg Depression Rating Scale; MMSE = Mini-Mental State Examination; TRD = treatment-resistant depression.
*Values are mean ± standard deviation or %.
†*p* values are uncorrected.

to a practical guide for estimating local gene expression levels in the cerebral cortex (more details are provided in Appendix 1).[43] Then, we classified the genes according to the data of Zeisel and colleagues[44] using single-cell RNA from the somatosensory cortex and cornu ammonis 1 region of the hippocampus in mice, specific to 1 of the 9 cell types: ependymal cells, oligodendrocytes, microglial cells, cornu ammonis 1 pyramidal neurons, interneurons, endothelial cells, somatosensory cortex pyramidal neurons, astrocytes and mural cells expressed in the cortex.

To correlate cell-specific gene expression profiles with TEP-derived altered signal propagation metrics, we analyzed the difference in signal propagation between the 2 study groups indexed by t value in each region. First, we applied source reconstruction to the 34 regions of the Desikan–Killiany atlas as described above. Then, we calculated the ERSPs for each brain region as described above. Finally, we calculated the differences in ERSP between the 2 study groups using t tests (ERSP of healthy controls v. ERSP of patients with TRD in each of the 34 regions). Then, we adapted the time–frequency window in which we found significant differences in ERSP for all electrodes (with cluster-based analysis) to ERSPs for each of the 34 regions. We then extracted the differences in averaged ERSP in the time window as t values.

As described above, we calculated cell-specific gene expression profiles and differences in ERSP (i.e., altered signal propagation profiles) for each region. Then, we tested the association between the interregional profiles of cell-specific gene expression and the interregional profiles of altered signal propagation using a resampling-based approach based on methods previously described.[27,28] We estimated significant average correlations between gene expression and altered signal propagation for each cell type panel separately using the distribution pattern from the random sampling. A rationale for this was that if specific cell types contribute to differences in altered signal propagation levels, the average correlation coefficients between gene expression and altered signal propagation levels for the genes of each cell type should be significantly different from those for a random set of genes. We evaluated the significance of the average correlations between gene expression and altered signal propagation for each cell type using an empirical null distribution of correlation coefficients between random genes and the signal propagation profile (repeated 1 million times). We then used the proportion of average correlation coefficients for each cell type that exceeded the null distribution correlation coefficients to calculate a 2-sided p value. We applied Bonferroni correction to control for the multiple comparisons. We set significance of the model at $\alpha = 0.0056$ (0.05/9 cells).

Results

Demographic data

A total of 90 participants were included in the present study: 60 patients with TRD and 30 healthy controls. Age and sex were well matched between the 2 groups. Participants' demographic data are presented in Table 1. The number of participants who had psychiatric comorbidities or a history of other psychiatric diagnosis is shown in Appendix 1.

Sensor-based power analysis

Single-pulse TMS for the dlPFC produced characteristic butterfly TEP plots for both groups (patients with TRD and healthy controls; Figure 2). The results of power analysis obtained from the sensor-based analysis are shown in Appendix 1, Figure S1. We observed no significant differences between the 2 groups in GMFP or LMFP.

Sensor-based time–frequency analysis

The results for ERSP and evoked power calculated by sensor-based time–frequency analysis are shown in Figure 3. The mean ERSP for all electrode sites and the local ERSP for the dlPFC stimulation site were decreased in the θ band in patients with TRD compared to healthy controls 200 to 400 ms after TMS (all electrodes, $p = 0.019$, uncorrected; dlPFC stimulation site, $p = 0.017$, uncorrected; $\alpha = 0.05$). The mean evoked power for all electrode sites was also decreased in patients with TRD compared to healthy controls ($p = 0.039$, uncorrected; $\alpha = 0.05$; Appendix 1, Figure S2A). We observed no significant difference between the 2 study groups for local evoked power (i.e., dlPFC stimulation site; $p = 0.30$, uncorrected; $\alpha = 0.05$; Appendix 1, Figure S2B).

For clusters that were significant, we performed post hoc tests on the individual mean power values calculated within

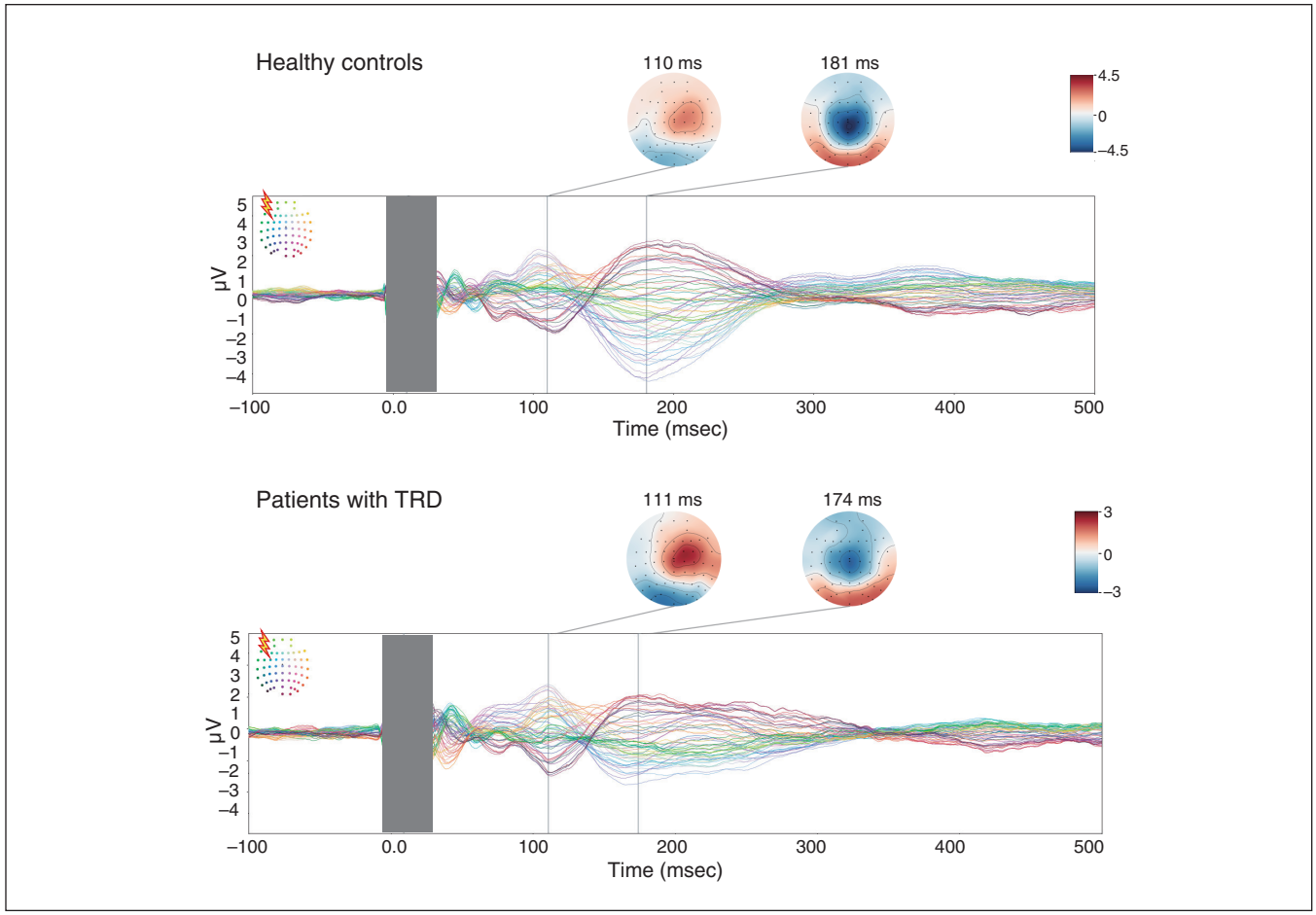

Fig. 2: Butterfly plots of the TEP waveforms among healthy controls (top) and patients with TRD (bottom). The TMS post-stimulus interval (–5 to 30 ms) is shown as a grey bar because of data cut-offs. Topoplots corresponding to the N100 and P180 components of the TEP are shown alongside the butterfly plots for both groups. In the butterfly plots, the colour of each waveform corresponds to the electrode colour diagram in the upper left corner, and the yellow symbols indicate TMS stimulation sites. TEP = TMS-evoked potential; TMS = transcranial magnetic stimulation; TRD = treatment-resistant depression.

the clusters. The *t* tests revealed a significant reduction of each mean power (ERSP of all electrodes, $t_{88} = 3.23$, $p = 0.002$; ERSP of dlPFC stimulation site, $t_{88} = 3.02$, $p = 0.004$; evoked power of all electrodes, $t_{88} = 3.16$, $p = 0.002$).

Source-based current density time-series analysis

Results for the current density time series obtained from the source-based analysis are shown in Appendix 1, Figure S3. We found no significant difference in current density between the 2 study groups in the source-based analysis.

Source-based time–frequency analysis

Results for the time–frequency current density distribution of ERSP and evoked power obtained from the source-based analysis are shown in Appendix 1, Figure S4. We found no difference in ERSP between the 2 study groups.

On the other hand, evoked power in the salience network was decreased in patients with TRD compared to healthy controls from 100 to 500 ms after TMS in the θ and α bands (salience network: $p = 0.0055$, uncorrected; $\alpha = 0.0071$; Figure 4). Evoked power in most of the other networks was also decreased in patients with TRD compared to healthy controls at a trend level (visual network, $p = 0.021$, uncorrected; somatosensory network, $p = 0.041$, uncorrected; dorsal attention network, $p = 0.0089$, uncorrected; limbic network, $p = 0.026$, uncorrected; and frontoparietal network, $p = 0.020$, uncorrected; $\alpha = 0.0071$), but not the default mode network ($p = 0.185$, uncorrected; $\alpha = 0.0071$; Appendix 1, Figure S5).

For the clusters of evoked power in the salience network that were significant, we performed post hoc tests on the individual mean power values calculated within the cluster. The *t* tests revealed a significant reduction of mean power ($t_{88} = 3.70$, $p = 0.0005$).

Cell-specific gene expression analysis

The interregional associations between the gene expression of specific cell types and altered signal propagation from the left

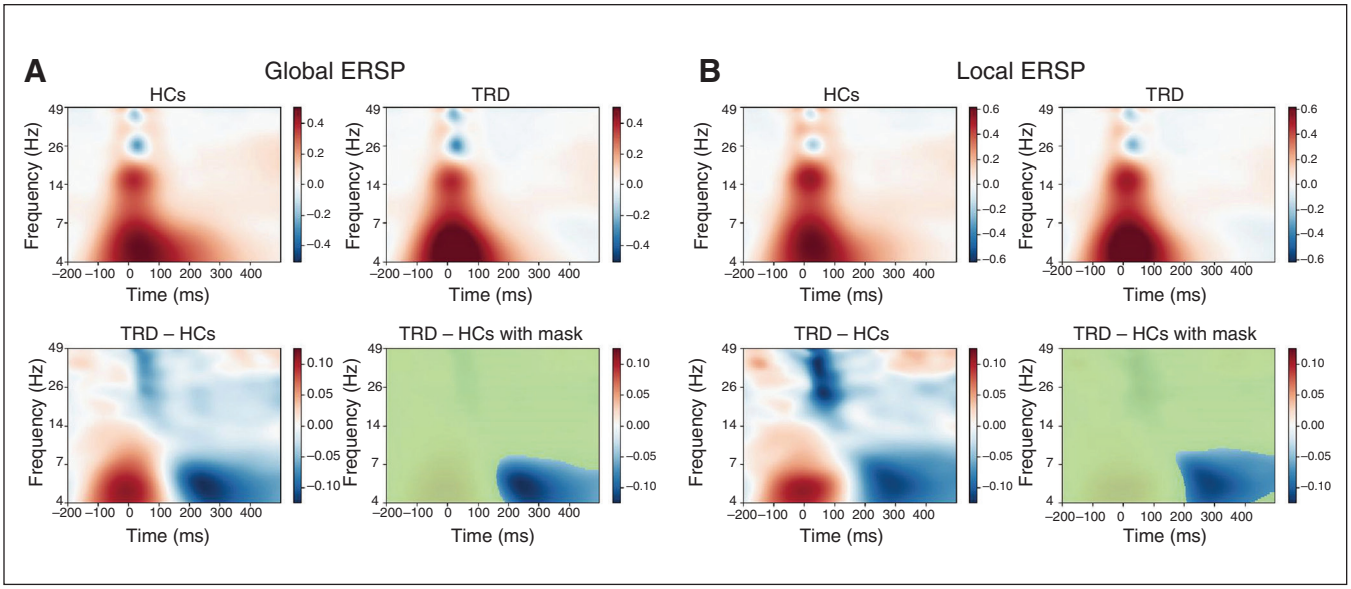

Fig. 3: Time–frequency analyses with ERSP. (A) ERSP from all electrode sites. (B) ERSP from electrodes corresponding to the stimulation site (i.e., left dlPFC). The ERSPs elicited by single-pulse TMS are shown for healthy controls in the upper left, and for patients with TRD in the upper right. Differences between the 2 groups are shown in the lower left. Areas with no significant differences between groups on the 2-dimensional cluster-level permutation tests are shown by green masks in the lower right. In each condition, the ERSPs for patients with TRD were significantly lowered in the θ band compared to healthy controls (all electrodes: $p = 0.019$, uncorrected; stimulation site (left dlPFC): $p = 0.017$, uncorrected; $\alpha = 0.05$). dlPFC = dorsolateral prefrontal cortex; ERSP = event-related spectral perturbation; HC = healthy control; TMS = transcranial magnetic stimulation; TRD = treatment-resistant depression.

dlPFC are presented in Figure 5. Mean correlation coefficients for each of the following cell types differed from the empirical null distributions: oligodendrocytes ($p < 0.000001$, uncorrected; $\alpha = 0.0056$; average correlation coefficient 0.13, 95% CI –0.0170 to 0.0392); cornu ammonis 1 pyramidal neurons ($p < 0.000001$, uncorrected; $\alpha = 0.0056$; average correlation coefficient –0.077, 95% CI –0.0189 to 0.0413); somatosensory cortex pyramidal neurons ($p = 0.00003$, uncorrected; $\alpha = 0.0056$; average correlation coefficient –0.033, 95% CI –0.0266 to 0.0491); and interneurons ($p < 0.000001$, uncorrected; $\alpha = 0.0056$; average correlation coefficient –0.048, 95% CI = –0.0209 to 0.0431). We found no significant difference in the other cell types after correcting for multiple comparisons (ependymal cells, $p = 0.0353$, uncorrected; microglial cells, $p = 0.0288$, uncorrected; endothelial cells, $p = 0.0069$, uncorrected; astrocytes, $p = 0.1312$, uncorrected; and mural cells, $p = 0.59$, uncorrected; $\alpha = 0.0056$).

Discussion

In the present study, we investigated signal propagation from the left dlPFC to other brain regions in patients with TRD compared to healthy controls using TMS-EEG-MRI. We also explored the role of the gene expression of specific cell types that may be strongly associated with impairment of signal propagation in patients with TRD using the Allen Human Brain Atlas data set. Our findings were 2-fold: that signal propagation from the left dlPFC to the salience network was reduced in the θ and α bands at 100 to 500 ms after TMS in patients with TRD; and that decreased signal propagation in patients with TRD was positively correlated with the gene expression of oligodendrocytes and negatively correlated with the gene expression of cornu ammonis 1 pyramidal neurons, somatosensory cortex pyramidal neurons and interneurons. Taken together, these results suggest that reduced signal propagation from the left dlPFC to the salience network may be a pathophysiological endophenotype of TRD that could be linked to the reduced expression of oligodendrocytes.

The strengths of the present study are as follows. First, it included a large sample of participants. Second, this was the first study to use individual MRI and high-density electrode EEG — with spatial information about the head and brain individually digitized — to develop precise source estimates of TMS-evoked EEG activity and perform time–frequency analysis on the signal source-estimated data in patients with TRD. Third, we used a virtual-histology approach for the first time to explore the relationships between signal propagation computed from the TMS-EEG measures and the degree of gene expression, leveraging the Allen Human Brain Atlas data set.

The salience network is involved in the detection of prominent external and internal stimuli and the orientation of attention to these stimuli,[45] whereas salience network dysfunction is implicated in the pathophysiology of depression through emotional over-reactivity.[46] The salience network is composed primarily of the anterior insula and the dorsal anterior cingulate cortex. We found that patients with TRD showed reduced signal propagation from the left dlPFC to this network, consistent with previous studies: patients with MDD showed reduced functional connectivity between the dlPFC and dorsal anterior cingulate cortex compared to

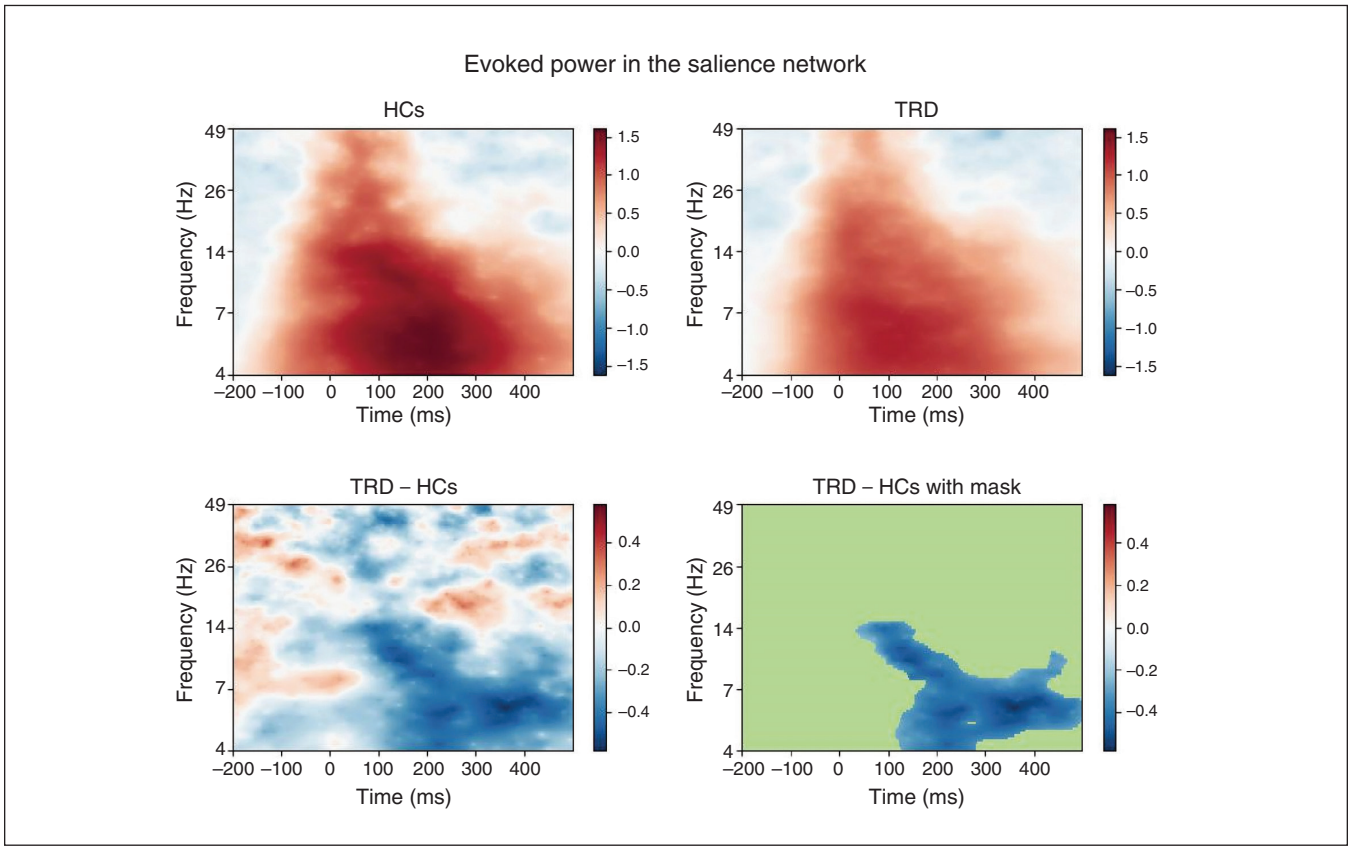

Fig. 4: Source-based time–frequency analyses with evoked power in the salience network. Evoked power is shown for healthy controls in the upper left, and for patients with TRD in the upper right. Differences in evoked power between the 2 groups are shown in the lower left. Areas with no significant differences between groups on the 2-dimensional cluster-level permutation tests are shown by green masks in the lower right. Evoked power in patients with TRD was significantly lower than in healthy controls (p = 0.005, uncorrected; α = 0.007). HC = healthy control; TRD = treatment-resistant depression.

healthy controls,[47] and patients with TRD showed reduced functional connectivity between the dlPFC and anterior insula compared to treatment responders.[48]

Given that rTMS can reduce hyperactive functional connectivity in the salience network in patients with TRD,[12] the signals from the left dlPFC to the salience network may be relatively attenuated, resulting in an uninhibited salience network, overactivity and more severe depressive symptoms. However, it is difficult to determine from the results of the present study alone whether the reduction in signal propagation from the left dlPFC to the other brain networks represents a long-term potentiation-like or long-term depression-like neuroplastic change in depression-related neural networks. Furthermore, our finding that signal propagation from the left dlPFC to the salience network was reduced by 5 to 15 Hz in patients with TRD was also in line with the fact that 10 Hz rTMS treatment to the left dlPFC in TRD has a robust therapeutic effect.[8,49,50] Thus, both neural networks and frequency bands may be closely related in the therapeutic mechanism of rTMS in depression. In other words, reduced signal propagation in the θ and α bands from the left dlPFC to the salience network may reflect an underlying pathophysiology in TRD through which rTMS exerts its corrective therapeutic effect.

The salience network was the only network with a significant reduction in signal propagation from the left dlPFC; however, several other networks showed a trend toward decrease (not the default mode network). These findings suggest that signal propagation from the left dlPFC is widely reduced in patients with TRD, but propagation to the salience network is most marked.

Dysfunction of oligodendrocytes has been implicated in the pathogenesis of depression.[24] Using microarray analysis of postmortem tissue in patients with MDD compared to healthy controls, Aston and colleagues[51] revealed that the expression of genes related to oligodendrocyte function was decreased. Given that brain regions with high baseline expression of disorder-linked genes are more susceptible over the course of the disease,[52] the function of oligodendrocytes is more likely to be affected in these neural networks, leading to dysfunction of signal propagation as indexed in the present study. Our finding of a significant association between the interregional profiles of oligodendrocyte-related gene expression in healthy controls and the interregional profiles of reduced signal propagation in patients with TRD was in line with this context. It has been reported that antidepressant administration restored lost white matter volume in patients

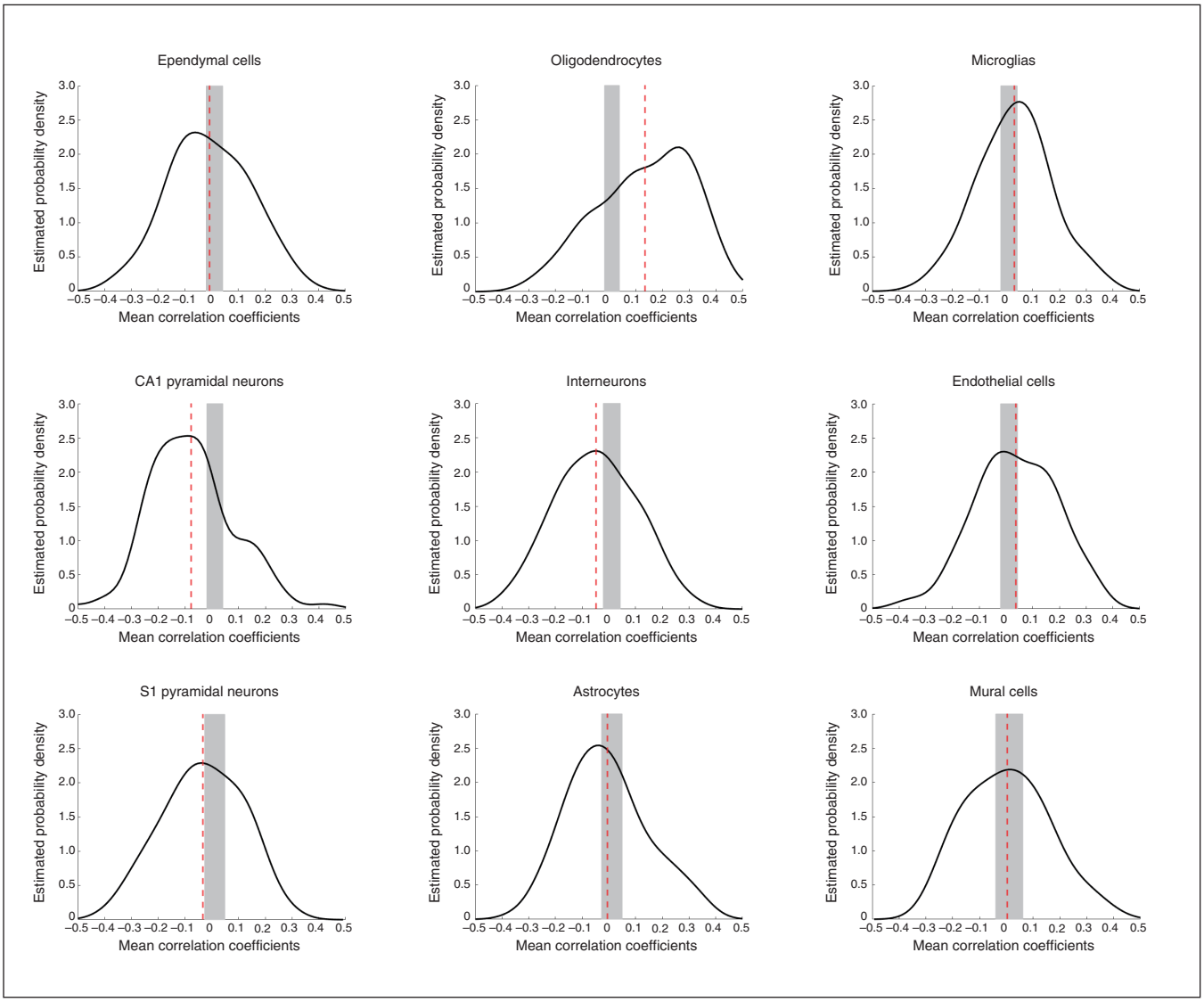

Fig. 5: Mean correlation coefficients for the degree of gene expression and altered TMS-EEG signal propagation in corresponding interregional profiles. We evaluated the significance of the average interregional correlations between gene expression and altered signal propagation for each cell type, compared to an empirical null distribution of correlation coefficients between the expression profiles of random gene sets and the signal propagation profile. The black line indicates the estimated probability density function for the correlation coefficients between each cell-type gene expression level and the signal propagation profiles from our data. The lower and upper cut-off for significance is indicated by the vertical edges of the shaded grey box. The mean correlation coefficients for each cell type are indicated by dashed red lines. The following cell types differed significantly from the empirical null distributions, even after correcting for multiple comparisons (p values uncorrected): oligodendrocytes ($p < 0.000001$; $\alpha = 0.0056$); CA1 pyramidal neurons ($p < 0.000001$; $\alpha = 0.0056$); S1 pyramidal neurons ($p = 0.00003$; $\alpha = 0.0056$); and interneurons ($p < 0.000001$; $\alpha = 0.0056$). CA1 = cornu ammonis 1; TMS = transcranial magnetic stimulation; S1 = somatosensory cortex.

with depression, and that antidepressants were less effective in patients with depression who had severe reductions in white matter volume.[53–55] Taken together, these results suggest that TRD may be the result of a decrease in signal propagation within and between specific neural networks, possibly because of oligodendrocyte dysfunction.

The present study showed that time–frequency analysis robustly revealed differences in signal propagation between the 2 study groups that were not evident in a power analysis of TEP. Unlike TEP power analysis, time–frequency analysis can decompose neural activity into finer frequencies, allowing for more accurate analysis and highlighting individual differences. As such, time–frequency analysis is more suitable for TMS-EEG measures with the dlPFC as the stimulation site.

ERSP is the index of time-locked activities (including phase-locked and non–phase-locked activity), whereas evoked power is the index of phase-locked activity only. In sensor-based analysis, activity is perceived as the sum of various activities — not just activity directly below the electrode — because of the influence of volume conductance and other factors. In contrast,

source-based analysis extracts only the activity of a specific region or network to detect signals with higher purity than sensor-based analysis. Consistent with this difference, we found that ERSP activity was strongly observed in the sensor-based analysis, and evoked power was strongly observed in the source-based analysis. Our source-based time–frequency analysis allowed us to depict neural activity with higher accuracy compared to the sensor-based TEP power analysis.

Limitations

This study had several limitations. First, because this study included only patients with TRD who were currently experiencing depressive symptoms, it was not possible to determine whether the findings were state or trait markers of TRD. Second, because TMS also elicits neural input from cutaneous sensation, the evoked activity obtained in this study (which was not compared with sham stimulation) did not necessarily originate from the firing of the left dlPFC (the site of stimulation). Third, the effects of antidepressants may have been implicated in the differences in TEP between the patients with TRD and the healthy controls. Antiepileptic drugs and benzodiazepines have some effects on TMS neurophysiological measures, but studies of the effects of antidepressants are limited, and no study has examined their effects on time–frequency analysis.[56] Therefore, we cannot completely rule out the possibility that antidepressants might have influenced the TMS-EEG results in the present study. Finally, because we stimulated only the left dlPFC, the present study might have evaluated only part of the pathophysiological basis for TRD. In the future, a more comprehensive analysis using TMS to the right dlPFC and other brain regions as probes will provide a more detailed understanding of the pathophysiology of TRD.

Conclusion

The findings of the present study suggest that signal propagation from the left dlPFC to the salience network in patients with TRD was reduced in θ and α bands compared to healthy controls, and that this reduction may be associated with decreased gene expression of oligodendrocytes. These results suggest that a refined assessment of signal propagation from the left dlPFC to other brain regions or networks might be useful for biotyping TRD. The development of novel neuromodulatory therapies based on these neurophysiological profiles might further progress TRD treatment strategies.

Affiliations: From the Department of Neuropsychiatry, Keio University School of Medicine, Tokyo, Japan (Wada, Nakajima, Honda, Takano, Taniguchi, Tsugawa, Y. Mimura, Hattori, M. Mimura, Noda); the Multimodal Imaging Group, Research Imaging Centre, Centre for Addiction and Mental Health, Toronto, Ont. (Nakajima); Teijin Pharma Ltd., Tokyo, Japan (Takano); the Center for Evolutionary Cognitive Sciences, Graduate School of Art and Sciences, University of Tokyo, Tokyo, Japan (Koike); the Temerty Centre for Therapeutic Brain Intervention, Centre for Addiction and Mental Health, Toronto, Ont. (Zomorrodi, Blumberger); the Department of Psychiatry, Faculty of Medicine, University of Toronto, Toronto, Ont. (Zomorrodi, Blumberger); the Department of Psychiatry, Faculty of Health, University of California San Diego, San Diego, CA (Daskalakis).

Funding: Japan Society for the Promotion of Science (20K16503 and 18K15375).

Competing interests: M. Wada received manuscript fees or speakers' honoraria from Dainippon Sumitomo Pharma, Eisai and Takeda Pharmaceutical Co. Ltd. S. Koike received honoraria from Siemens Healthineers, Takeda Pharmaceutical Company Ltd. and Lundbeck Japan K.K. D. Blumberger receives research support from the Canadian Institutes of Health Research, the US National Institutes of Health, the Brain Canada Foundation and the Temerty Family through the CAMH Foundation and the Campbell Family Research Institute; has participated in advisory boards for Janssen and Welcony Inc; has received research support and in-kind equipment support for an investigator-initiated study from Brainsway Ltd.; was the site principal investigator for 3 sponsor-initiated studies for Brainsway Ltd.; received in-kind equipment support from Magventure for investigator-initiated studies; and received medication supplies for an investigator-initiated trial from Indivior. Z. Daskalakis received grants from Brainsway Inc. and Magventure Inc., and participated on an advisory board for Brainsway Inc. M. Mimura received grants from Shionogi, Takeda and Tanabe Mitsubishi outside the submitted work; and received speaker's honoraria from Dainippon-SumitomoPharma, Eli Lilly, Fuji Film RI Pharma, Janssen Pharmaceutical, Mochida Pharmaceutical, Otsuka Pharmaceutical, Pfizer, Shionogi, Takeda Yakuhin, Teijin Pharma and Viatris, outside the submitted work. No other competing interests declared.

Contributors: S. Nakajima and Y. Noda designed the study. S. Honda, M. Takano, K. Taniguchi, Y. Mimura, and N. Hattori acquired the data, which M. Wada, S. Tsugawa, S. Koike, R. Zomorrodi, D. Blumberger, Z. Daskalakis, M. Mimura and Y. Noda analyzed. M. Wada wrote the article, which S. Nakajima, S. Honda, M. Takano, K. Taniguchi, S. Tsugawa, Y. Mimura, N. Hattori, S. Koike, R. Zomorrodi, D. Blumberger, Z. Daskalakis, M. Mimura, and Y. Noda reviewed. All authors approved the final version to be published, agree to be accountable for all aspects of the work and can certify that no other individuals not listed as authors have made substantial contributions to the paper.

Registration: UMIN000028863

References

1. Bromet E, Andrade LH, Hwang I, et al. Cross-national epidemiology of DSM-IV major depressive episode. *BMC Med* 2011;9:90.
2. Gaynes BN, Lux LJ, Lloyd SW, et al. *Nonpharmacologic interventions for treatment-resistant depression in adults*. Rockville (MD): Agency for Healthcare Research and Quality; 2011.
3. Jaffe DH, Rive B, Denee TR. The humanistic and economic burden of treatment-resistant depression in Europe: a cross-sectional study. *BMC Psychiatry* 2019;19:247.
4. Kaiser RH, Andrews-Hanna JR, Wager TD, et al. Large-scale network dysfunction in major depressive disorder: a meta-analysis of resting-state functional connectivity. *JAMA Psychiatry* 2015;72:603-11.
5. Mulders PC, van Eijndhoven PF, Schene AH, et al. Resting-state functional connectivity in major depressive disorder: a review. *Neurosci Biobehav Rev* 2015;56:330-44.
6. Dichter GS, Gibbs D, Smoski MJ. A systematic review of relations between resting-state functional-MRI and treatment response in major depressive disorder. *J Affect Disord* 2015;172:8-17.
7. Runia N, Yücel DE, Lok A, et al. The neurobiology of treatment-resistant depression: a systematic review of neuroimaging studies. *Neurosci Biobehav Rev* 2022;132:433-48.
8. Somani A, Kar SK. Efficacy of repetitive transcranial magnetic stimulation in treatment-resistant depression: the evidence thus far. *Gen Psychiatr* 2019;32:e100074.

9. Alkhasli I, Sakreida K, Mottaghy FM, et al. Modulation of frontostriatal functional connectivity using transcranial magnetic stimulation. *Front Hum Neurosci* 2019;13:190.
10. Weigand A, Horn A, Caballero R, et al. Prospective validation that subgenual connectivity predicts antidepressant efficacy of transcranial magnetic stimulation sites. *Biol Psychiatry* 2018;84:28-37.
11. Hadas I, Zomorrodi R, Hill AT, et al. Subgenual cingulate connectivity and hippocampal activation are related to MST therapeutic and adverse effects. *Transl Psychiatry* 2020;10:392.
12. Godfrey KEM, Muthukumaraswamy SD, Stinear CM, et al. Decreased salience network fMRI functional connectivity following a course of rTMS for treatment-resistant depression. *J Affect Disord* 2022;300:235-42.
13. Smart O, Choi KS, Riva-Posse P, et al. Initial unilateral exposure to deep brain stimulation in treatment-resistant depression patients alters spectral power in the subcallosal cingulate. *Front Comput Neurosci* 2018;12:43.
14. Tremblay S, Rogasch NC, Premoli I, et al. Clinical utility and prospective of TMS–EEG. *Clin Neurophysiol* 2019;130:802-44.
15. Romero MC, Davare M, Armendariz M, et al. Neural effects of transcranial magnetic stimulation at the single-cell level. *Nat Commun* 2019;10:2642.
16. Bortoletto M, Veniero D, Thut G, et al. The contribution of TMS–EEG coregistration in the exploration of the human cortical connectome. *Neurosci Biobehav Rev* 2015;49:114-24.
17. Rosanova M, Casarotto S, Pigorini A, et al. Combining transcranial magnetic stimulation with electroencephalography to study human cortical excitability and effective connectivity. *Neuronal Network Analysis* 2011;67:435-57.
18. Granö I, Mutanen TP, Tervo AE, et al. Local brain-state dependency of effective connectivity: evidence from TMS–EEG. *bioRxiv* 2021. doi:10.1101/2021.10.01.462795
19. Massimini M, Ferrarelli F, Huber R, et al. Breakdown of cortical effective connectivity during sleep. *Science* 2005;309:2228-32.
20. Sarasso S, Rosanova M, Casali AG, et al. Quantifying cortical EEG responses to TMS in (un)consciousness. *Clin EEG Neurosci* 2014;45:40-9.
21. Ozdemir RA, Tadayon E, Boucher P, et al. Individualized perturbation of the human connectome reveals reproducible biomarkers of network dynamics relevant to cognition. *Proc Natl Acad Sci U S A* 2020;117:8115-25.
22. Cullen CL, Senesi M, Tang AD, et al. Low-intensity transcranial magnetic stimulation promotes the survival and maturation of newborn oligodendrocytes in the adult mouse brain. *Glia* 2019;67:1462-77.
23. Buzsáki G, Schomburg EW. What does gamma coherence tell us about inter-regional neural communication? *Nat Neurosci* 2015;18:484-9.
24. Zhou B, Zhu Z, Ransom BR, et al. Oligodendrocyte lineage cells and depression. *Mol Psychiatry* 2021;26:103-17.
25. Moriguchi S, Takamiya A, Noda Y, et al. Glutamatergic neurometabolite levels in major depressive disorder: a systematic review and meta-analysis of proton magnetic resonance spectroscopy studies. *Mol Psychiatry* 2019;24:952-64.
26. Godfrey KEM, Gardner AC, Kwon S, et al. Differences in excitatory and inhibitory neurotransmitter levels between depressed patients and healthy controls: a systematic review and meta-analysis. *J Psychiatr Res* 2018;105:33-44.
27. Patel Y, Shin J, Gowland PA, et al. Maturation of the human cerebral cortex during adolescence: myelin or dendritic arbor? *Cereb Cortex* 2019;29:3351-62.
28. Shin J, French L, Xu T, et al. Cell-specific gene-expression profiles and cortical thickness in the human brain. *Cereb Cortex* 2018;28:3267-77.
29. American Psychiatric Association. *Diagnostic and statistical manual of mental disorders. Fifth edition.* Arlington (VA): American Psychiatric Association; 2013.
30. Voineskos D, Blumberger DM, Zomorrodi R, et al. Altered transcranial magnetic stimulation-electroencephalographic markers of inhibition and excitation in the dorsolateral prefrontal cortex in major depressive disorder. *Biol Psychiatry* 2019;85:477-86.
31. Yeo BTT, Krienen FM, Sepulcre J, et al. The organization of the human cerebral cortex estimated by intrinsic functional connectivity. *J Neurophysiol* 2011;106:1125-65.
32. Rossi S, Hallett M, Rossini PM, et al. Safety, ethical considerations, and application guidelines for the use of transcranial magnetic stimulation in clinical practice and research. *Clin Neurophysiol* 2009;120:2008-39.
33. Delorme A, Makeig S. EEGLAB: an open source toolbox for analysis of single-trial EEG dynamics including independent component analysis. *J Neurosci Methods* 2004;134:9-21.
34. Rogasch NC, Sullivan C, Thomson RH, et al. Analysing concurrent transcranial magnetic stimulation and electroencephalographic data: a review and introduction to the open-source TESA software. *Neuroimage* 2017;147:934-51.
35. Gramfort A, Luessi M, Larson E, et al. MEG and EEG data analysis with MNE-Python. *Front Neurosci* 2013;7:267.
36. Komssi S, Kähkönen S, Ilmoniemi RJ. The effect of stimulus intensity on brain responses evoked by transcranial magnetic stimulation. *Hum Brain Mapp* 2004;21:154-64.
37. Lehmann D, Skrandies W. Reference-free identification of components of checkerboard-evoked multichannel potential fields. *Electroencephalogr Clin Neurophysiol* 1980;48:609-21.
38. Casarotto S, Canali P, Rosanova M, et al. Assessing the effects of electroconvulsive therapy on cortical excitability by means of transcranial magnetic stimulation and electroencephalography. *Brain Topogr* 2013;26:326-37.
39. Maris E, Oostenveld R. Nonparametric statistical testing of EEG- and MEG-data. *J Neurosci Methods* 2007;164:177-90.
40. Smith SM, Nichols TE. Threshold-free cluster enhancement: addressing problems of smoothing, threshold dependence and localisation in cluster inference. *Neuroimage* 2009;44:83-98.
41. Hawrylycz MJ, Lein ES, Guillozet-Bongaarts AL, et al. An anatomically comprehensive atlas of the adult human brain transcriptome. *Nature* 2012;489:391-9.
42. French L, Paus T. A FreeSurfer view of the cortical transcriptome generated from the Allen Human Brain Atlas. *Front Neurosci* 2015; 9:323.
43. Arnatkeviciute A, Fulcher BD, Fornito A. A practical guide to linking brain-wide gene expression and neuroimaging data. *Neuroimage* 2019;189:353-67.
44. Zeisel A, Muñoz-Manchado AB, Codeluppi S, et al. Cell types in the mouse cortex and hippocampus revealed by single-cell RNA-seq. *Science* 2015;347:1138-42.
45. Seeley WW, Menon V, Schatzberg AF, et al. Dissociable intrinsic connectivity networks for salience processing and executive control. *J Neurosci* 2007;27:2349-56.
46. Hamilton JP, Chen MC, Gotlib IH. Neural systems approaches to understanding major depressive disorder: an intrinsic functional organization perspective. *Neurobiol Dis* 2013;52:4-11.
47. Aizenstein HJ, Butters MA, Wu M, et al. Altered functioning of the executive control circuit in late-life depression: episodic and persistent phenomena. *Am J Geriatr Psychiatry* 2009;17:30-42.
48. Yuan H, Zhu X, Tang W, et al. Connectivity between the anterior insula and dorsolateral prefrontal cortex links early symptom improvement to treatment response. *J Affect Disord* 2020;260:490-7.
49. Hua J, Wolff A, Zhang J, et al. Alpha and theta peak frequency track on- and off-thoughts. *Commun Biol* 2022;5:209.
50. Wolff A, de la Salle S, Sorgini A, et al. Atypical temporal dynamics of resting state shapes stimulus-evoked activity in depression — an EEG study on rest-stimulus interaction. *Front Psychiatry* 2019;10:719.
51. Aston C, Jiang L, Sokolov BP. Transcriptional profiling reveals evidence for signaling and oligodendroglial abnormalities in the temporal cortex from patients with major depressive disorder. *Mol Psychiatry* 2005;10:309-22.
52. Seidlitz J, Nadig A, Liu S, et al. Transcriptomic and cellular decoding of regional brain vulnerability to neurogenetic disorders. *Nat Commun* 2020;11:1-14.
53. Zeng LL, Liu L, Liu Y, et al. Antidepressant treatment normalizes white matter volume in patients with major depression. *PLoS One* 2012;7:e44248.
54. Serafini G, Pompili M, Borgwardt S, et al. The role of white matter abnormalities in treatment-resistant depression: a systematic review. *Curr Pharm Des* 2015;21:1337-46.
55. Peng HJ, Zheng HR, Ning YP, et al. Abnormalities of cortical-limbic-cerebellar white matter networks may contribute to treatment-resistant depression: a diffusion tensor imaging study. *BMC Psychiatry* 2013;13:72.
56. Ziemann U, Reis J, Schwenkreis P, et al. TMS and drugs revisited 2014. *Clin Neurophysiol* 2015;126:1847-68.